

Supporting Information

Epitaxial growth of light-responsive azobenzene molecular crystal actuators on oriented polyethylene films

Shaji Varghese^{a*}, Sebastian Fredrich^a, Ghislaine Vantomme^{a,b}, Sugosh R. Prabhu^c, Joan Teyssandier^c, Steven De Feyter^c, John Severn^{a,d}, C.W. M. Bastiaansen^{a,e}, and A. P. H. J. Schenning^{a,b*}

^aStimuli-responsive Functional Materials and Devices, Department of Chemical Engineering and Chemistry, Eindhoven University of Technology, Eindhoven, The Netherlands.

^bInstitute for Complex Molecular Systems, Eindhoven University of Technology, P.O. Box 513, 5600 MB, Eindhoven, The Netherlands.

^cDivision of Molecular Imaging and Photonics, Department of Chemistry, KU Leuven, Celestijnenlaan 200F, B 3001, Leuven, Belgium.

^dDSM Materials Science Center, NL-6160 MD Geleen, The Netherlands.

^eSchool of Engineering and Materials Science, Queen Mary, University of London, London, UK.

*E-mail: shajivar@gmail.com, A.P.H.J.Schenning@tue.nl

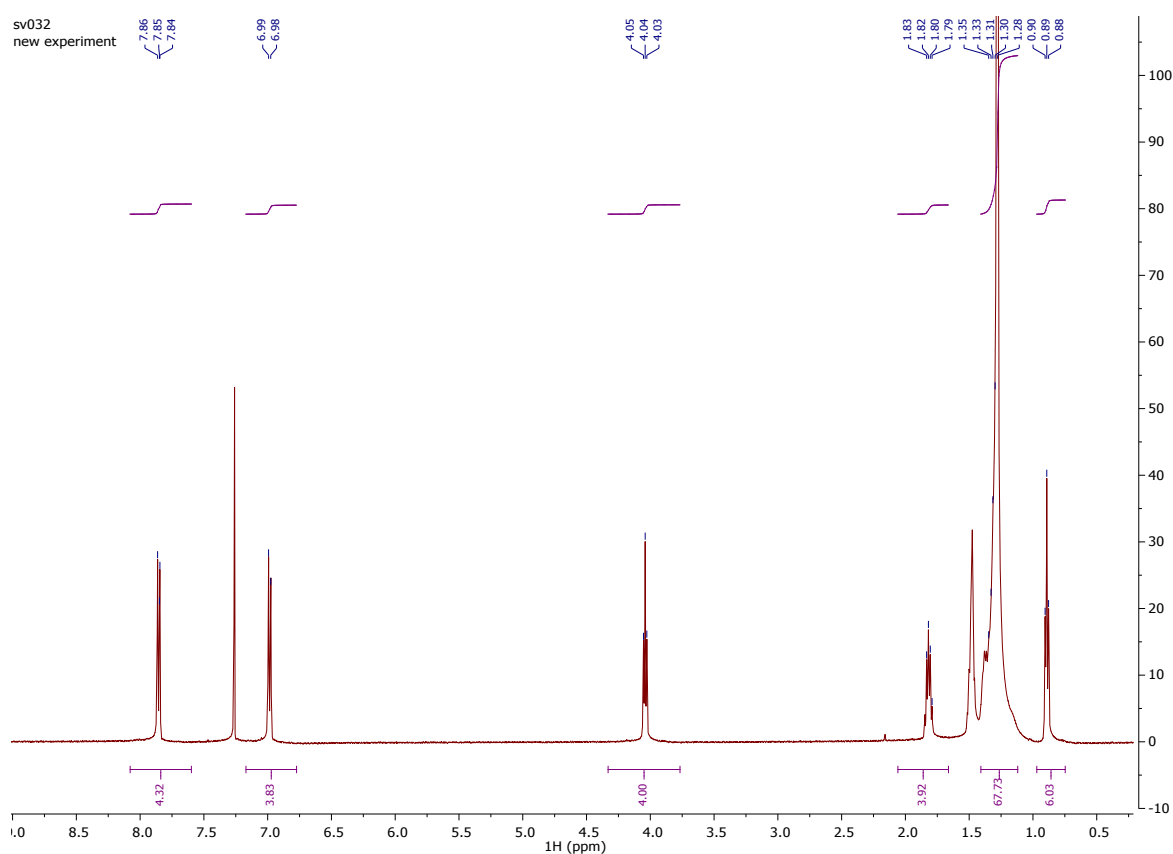


Figure S1: ¹H-NMR spectrum of **1**.

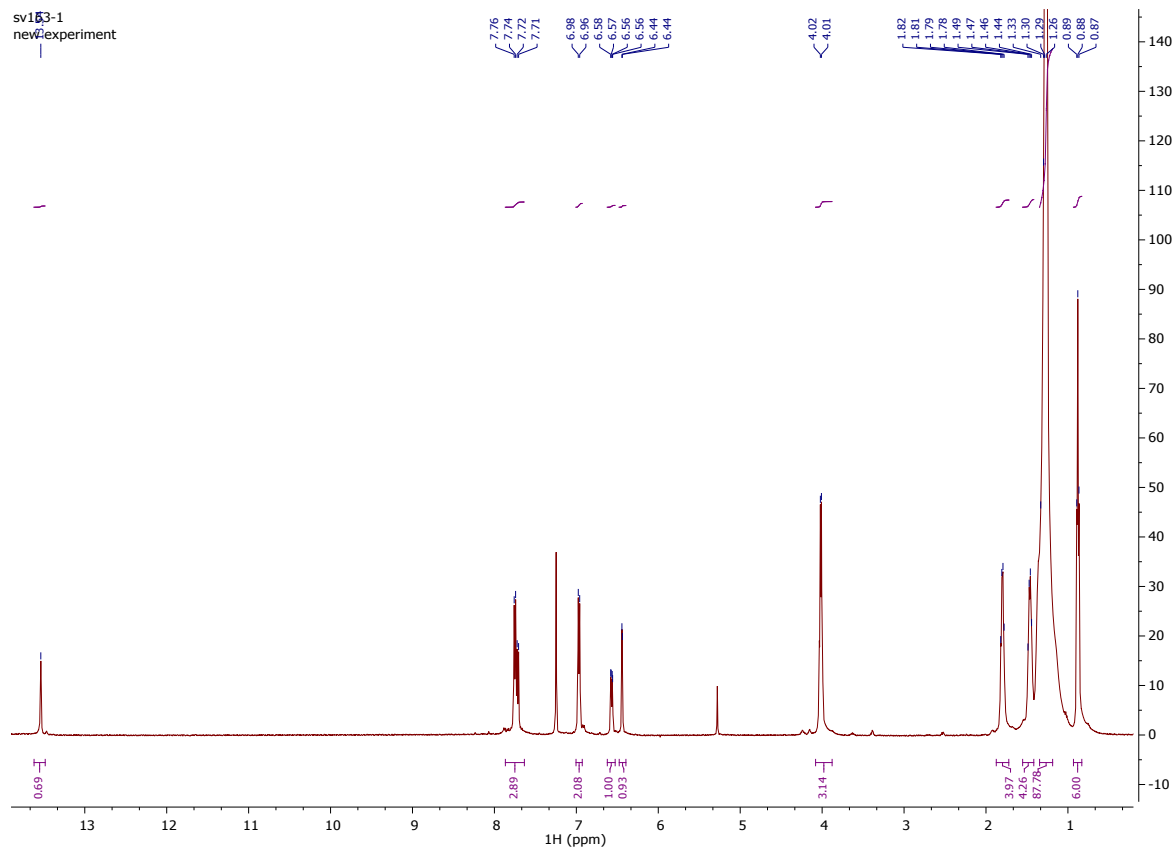


Figure S2: ^1H -NMR spectrum of **2**.

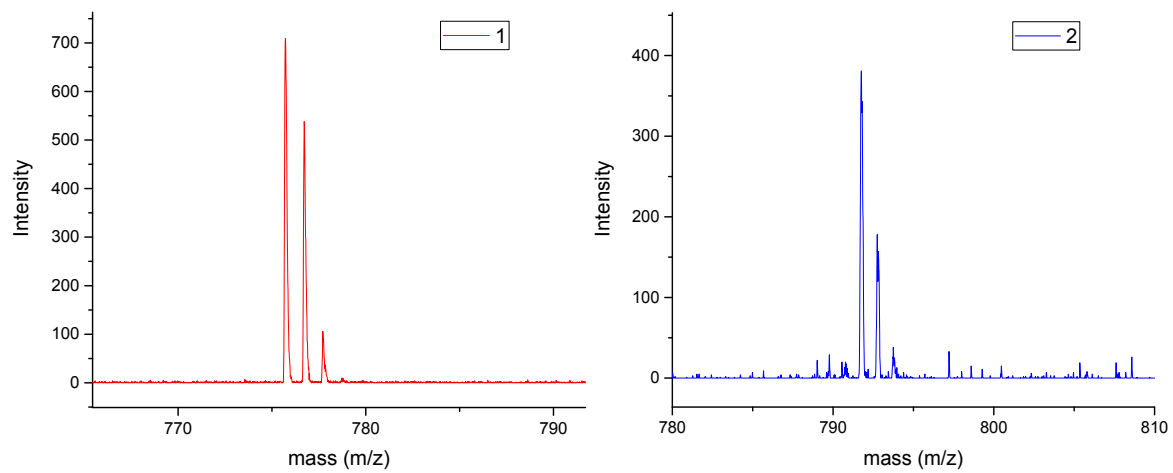


Figure S3: MALDI-TOF mass spectrum of **1** and **2**.

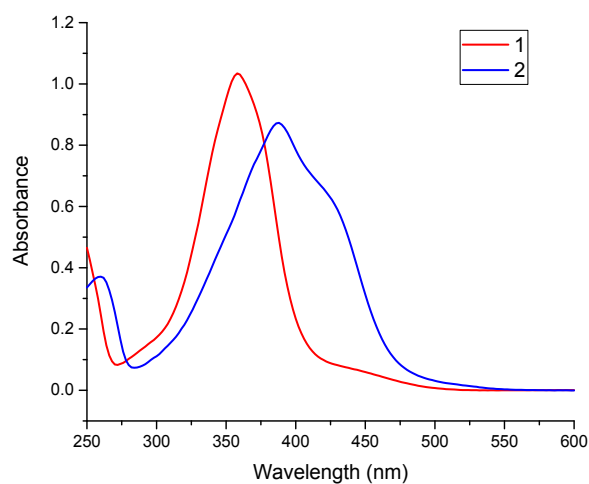


Figure S4: Absorption spectrum of **1** and **2** in CHCl_3 (40°C).

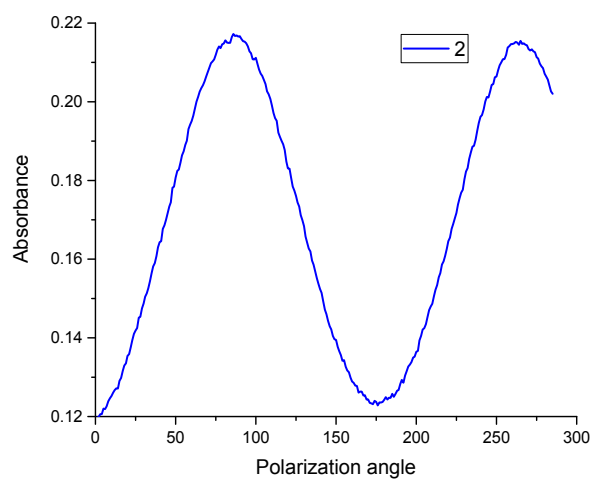


Figure S5: Polarised absorption spectrum of **2** on oriented UHMW-PE at $\lambda = 400$ nm.

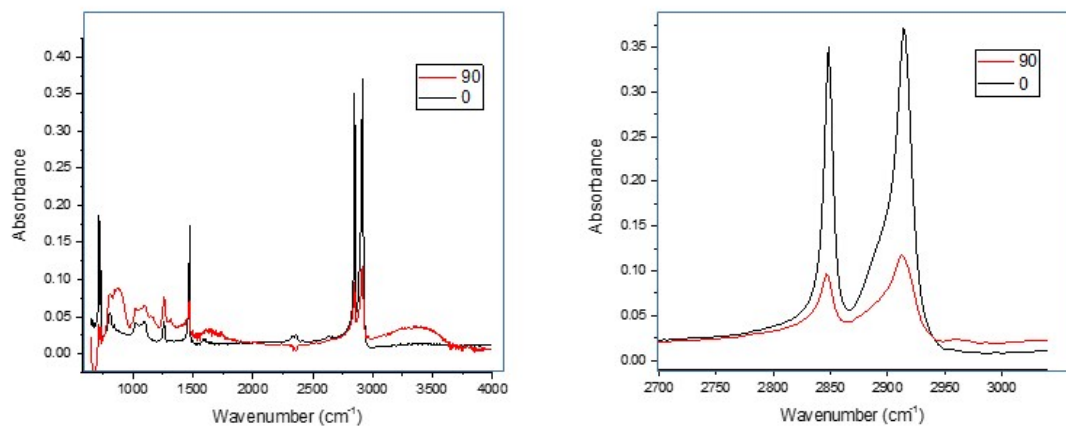


Figure S6: Polarised IR spectra of **2** on oriented UHMW-PE.

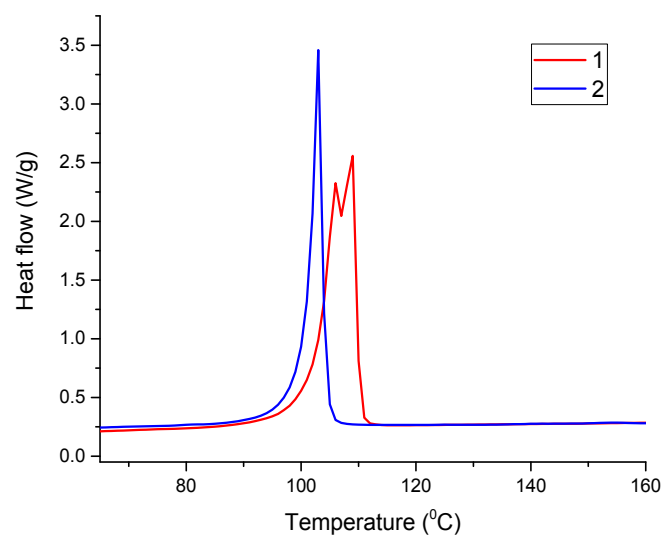


Figure S7: DSC trace of **1** and **2**.

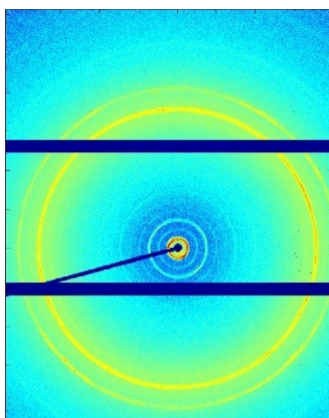


Figure S8: Wide angle X-ray (WAXS) diffraction pattern of **1**.

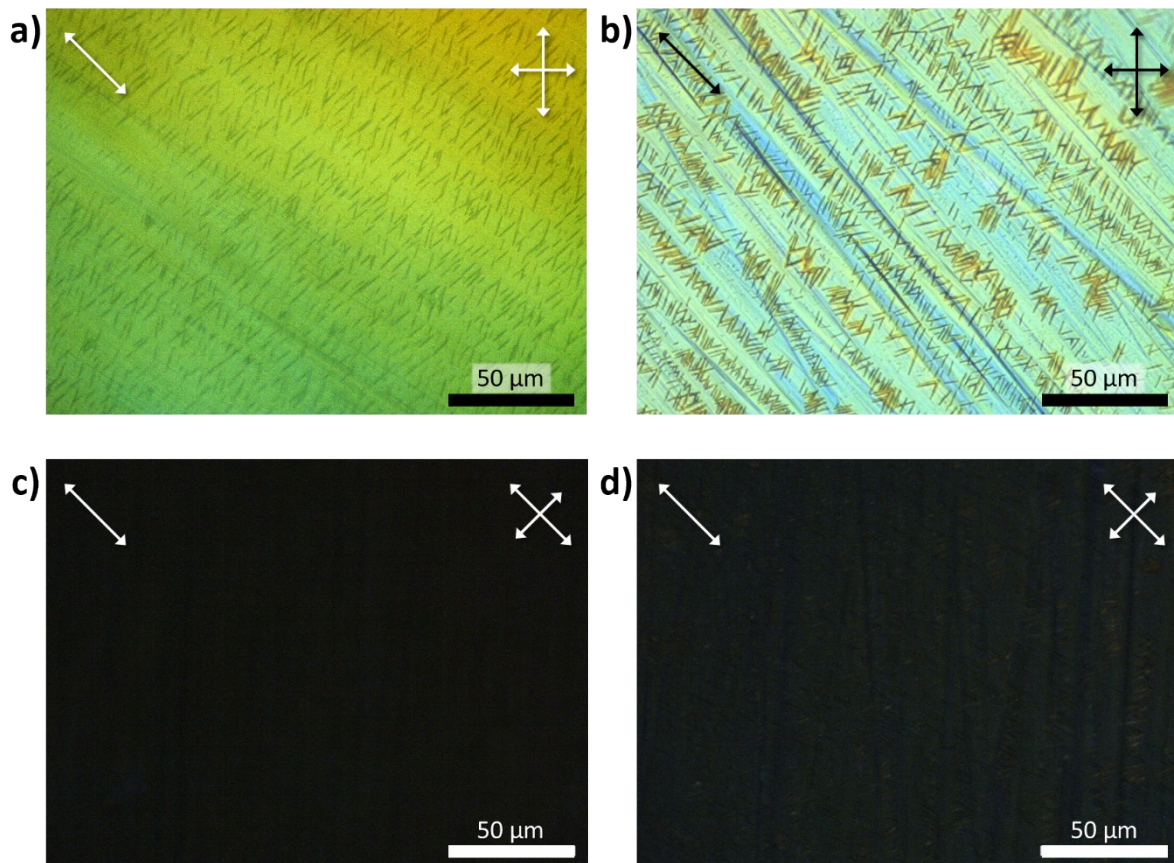


Figure S9: Optical micrograph of a) **1** on an oriented UHMW-PE film at 45° with regard to crossed polarisers; b) **2** on an oriented UHMW-PE film at 45° with regard to crossed polarisers; c) **1** on an oriented UHMW-PE film parallel to one crossed polariser; d) **2** on an oriented UHMW-PE film parallel to one to crossed polariser. The drawing directions are given in the top left, the polariser directions in the top right corners of the images.

Uniaxially drawn HDPE films¹

Isotropic HDPE sheets of approximately 1.5 mm thickness were obtained by compression molding at 160 °C for 5 min followed by quenching in water. Dumbbell shape like PE samples with gauge dimensions 1.2 x 0.2 cm were then cut from the compression molding sheet. These samples were subsequently drawn to a draw ratio (λ) of 15 at 80 °C in air using Zwick Z100 tensile tester at a cross speed of 100 mm/min. The draw ratio (λ) of 15 was determined from the displacement of ink mark which initially spaced at an interval of 1 mm on the PE film surface. The thickness of the PE film was calculated by weighing, assuming that density equals to 1 g/cm³.

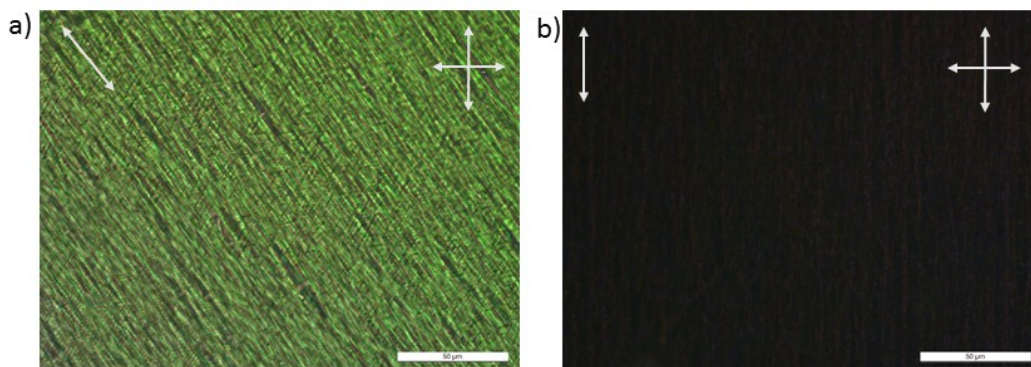


Figure S10: Polarised optical microscope (POM) micrographs of **1** on the surface of oriented HDPE. a) Drawing direction of PE is at an angle of 45° with regard to the crossed polarisers; b) Drawing direction of PE is parallel to one of the polarisers.

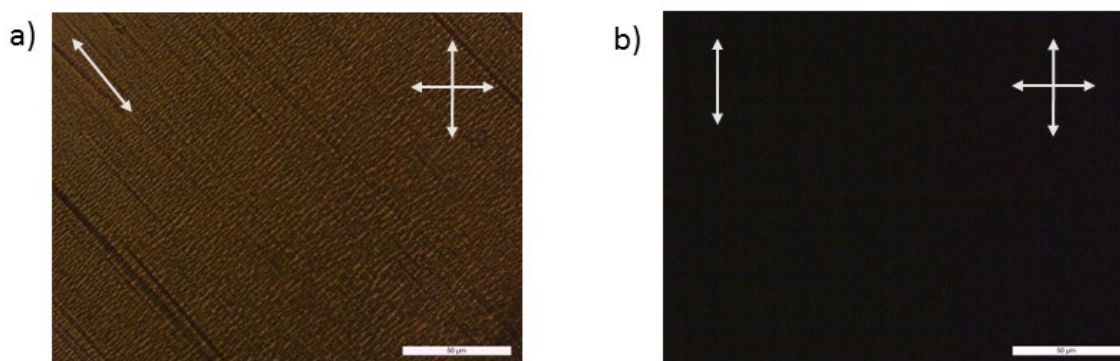


Figure S11: POM image of polyethylene wax 1000 on UHMW-PE. a) Drawing direction of PE is at an angle of 45° with regard to the crossed polarisers; b) Drawing direction of PE is parallel to one of the polarisers.

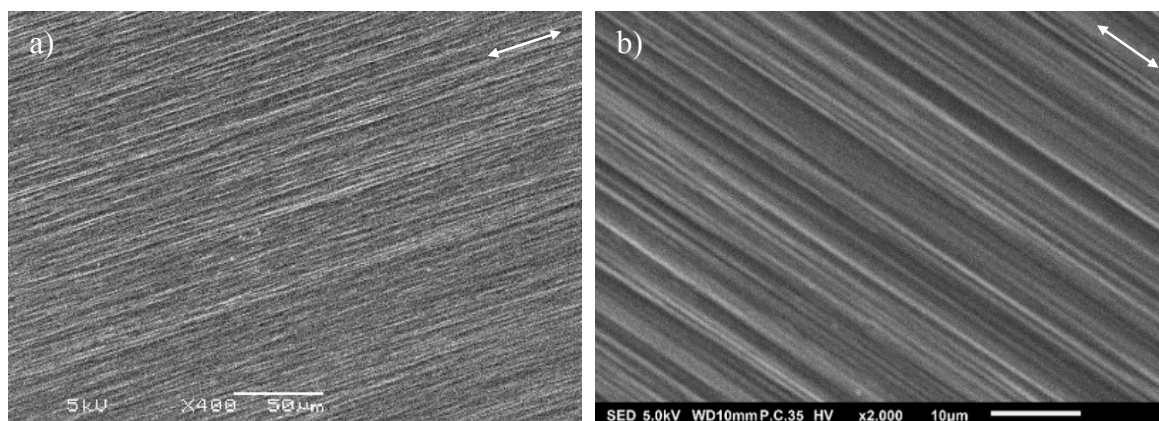


Figure S12: SEM images of uniaxially oriented a) HDPE b) UHMW-PE.

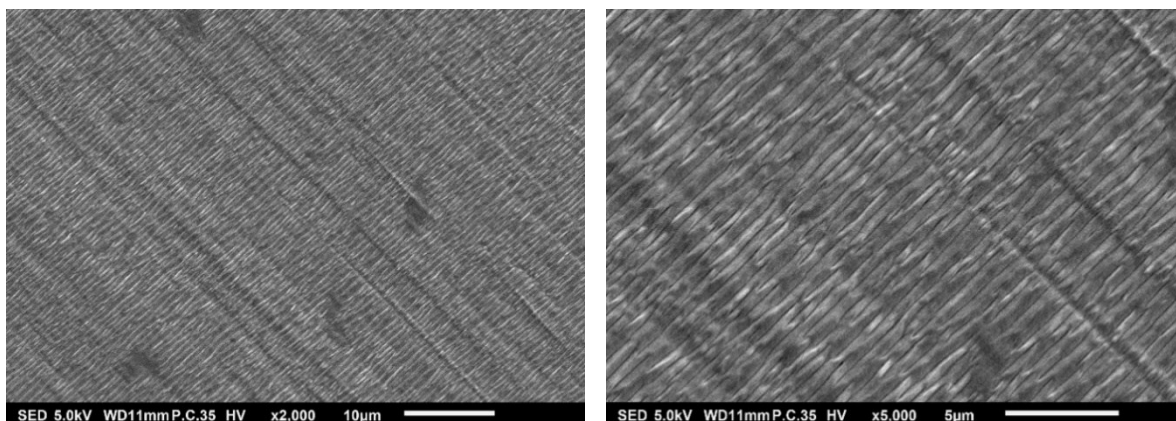


Figure S13: SEM images of polyethylene wax 1000 on oriented UHMW-PE.

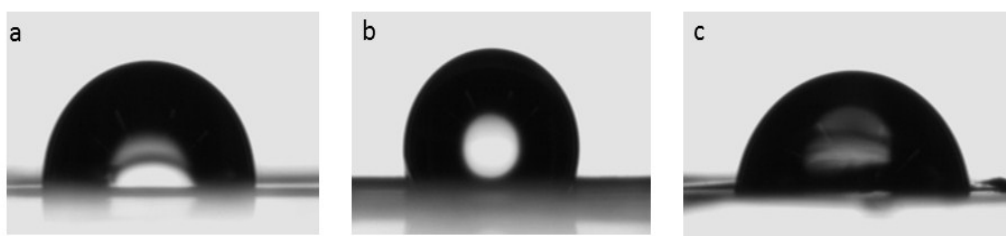


Figure S14: Water contact angles (CA) profile of the surface a) oriented UHMW-PE b) **1** on oriented UHMW-PE (107 ± 1) and c) **2** on oriented UHMW-PE (85 ± 1). The CA were measured with deionised water on a Dataphysics OCA30 instrument at room temperature. As expected epitaxial layer of **2** on oriented UHMW-PE is more hydrophilic than **1** on oriented UHMW-PE.

DMA measurements / stress strain measurements

The DMA-measurements were done on a Discovery DMA 850. All experiments were done at room temperature and under protection from ambient light. UHMWPE-samples of around 30 mm length and 5 mm width were clamped on both ends. The length of the free-hanging part was automatically measured by the machine and about 15 mm throughout the samples. To calculate the stress values, the samples were weighed to indirectly obtain the average height of the films. The films were subjected to a pre-stress of 0.3 N and a pre-strain of 1%, after which a constant strain was applied thereby inducing stress relaxation. This relaxation was monitored over time. The difference between the stress relaxation in the dark and under irradiation was used to plot the light-induced stress against the intensity of the light source. The light-induced stress for **1** and **2** on PE using 365 nm and 405 nm, respectively, was measured multiple times obtaining reproducible results.

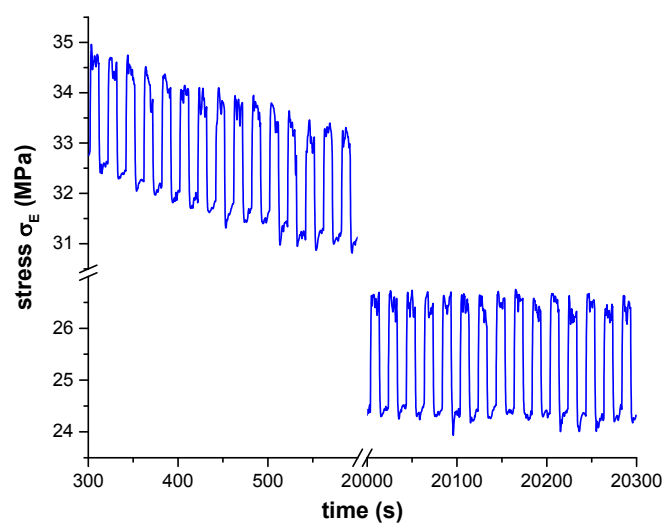


Figure 15: longterm stress relaxation experiment of UHMW-PE with crystals of **2** under alternating irradiation (365 nm) and darkness. Shape and intensity of the light-induced stress is not changing over 2000 cycles revealing a good reversibility and negligible fatigue of the actuator.

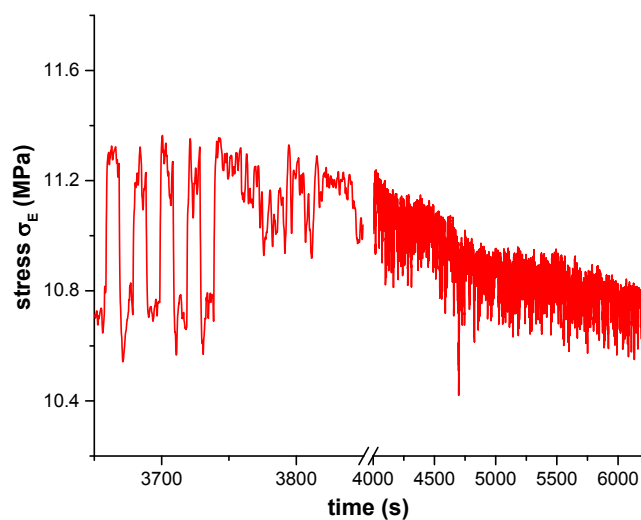


Figure 16: longterm stress strain experiment of UHMW-PE with crystals of **1** under constant irradiation (365 nm) over 1h. The intensity of the light-induced stress is not varying strongly and follows the same trend as in the dark state.

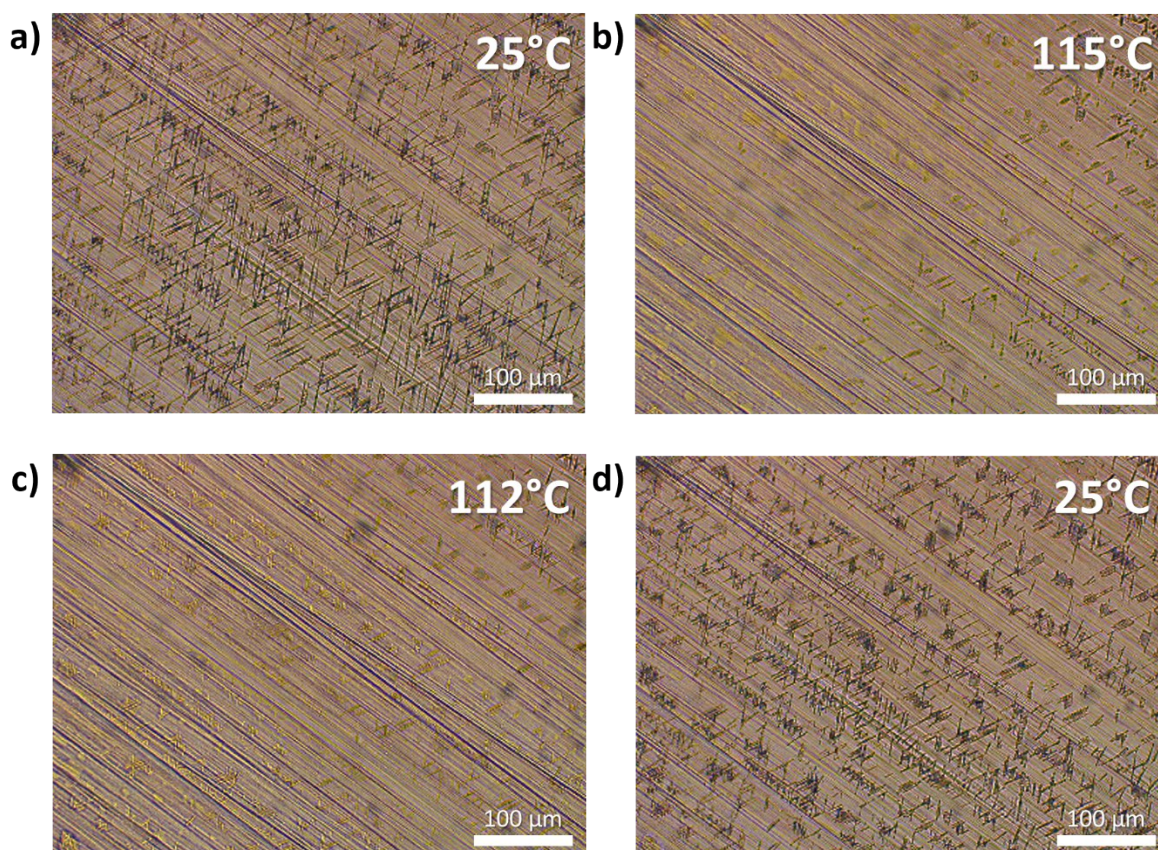


Figure 17: Optical microscopy images of **1** on UHMW-PE at a) 25 °C b) 115 °C c) cooling to 112 °C d) cooling back to 25 °C. Between taking the images b and c, the sample was heated to 118 °C to guarantee the melting of all crystals. The exact position of the crystallites changes during the cycle.

AFM and STM data

In order to confirm the results obtained by AFM and gain more insight into the organisation at the molecular level, STM analysis of **1** was performed. Since PE is not a suitable substrate for STM, imaging was performed at the 1-phenyloctane (1-PO)/HOPG interface. Alkane derivatives are known to grow epitaxially on HOPG, although the relation is a bit different compared to PE. The alkanes lie parallel to the three main symmetry axes of the graphite lattice.² High-resolution STM imaging (Figure S16a) revealed that a lamellar structure is also present on HOPG. However, the AFM analysis of **1** on oriented UHMW-PE showed a periodicity of approx. 6.2 nm, while it is roughly half this value (3.3 nm) on HOPG. A closer look into the columnar features allowed to identify the alkyl chains and propose the molecular model in Figure S16b. The periodicity of the lamellae corresponds to molecules assembled *via* interdigitation of their alkyl chains. The length of individual molecules of **1** can be measured both in the experimental images and on the model (approx. 6.25 nm) and furthermore suggests that on the stretched PE surface **1** crystallises in an end-to-end assembly. The differences between the assembly on the two surfaces can be explained by the molecule-surface interactions and the tendency for close-packing. On HOPG, π - π interactions between phenyl rings and graphite force the azobenzene units to lie flat on the surface (“face-on”). As a consequence, the maximisation of both the van der Waals interactions between alkyl chains

and the molecular density on the surface requires interdigitation between molecules of adjacent columns. On the PE surface, the azobenzenes are lying “edge-on”, which allows for end-to-end packing of the alkyl chains.

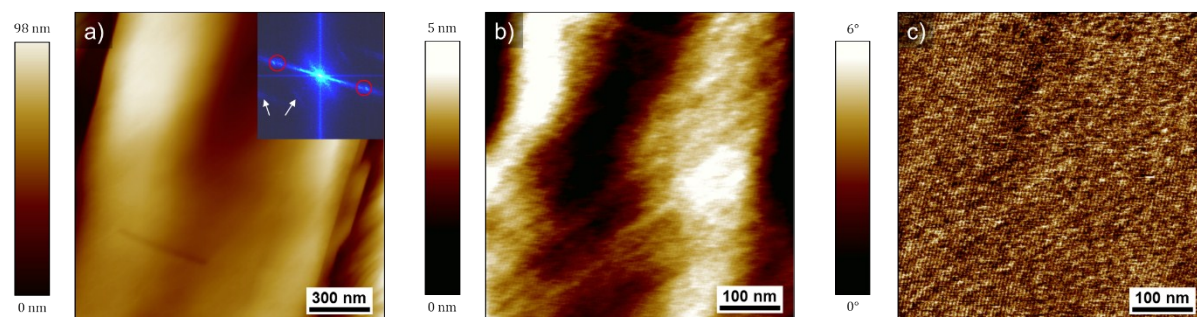


Figure S18: AFM images. a) Topography image of an epitaxially grown crystal of **2**. A Fourier transform of the corresponding phase image is shown in inset; the bright dots highlighted by the red circles show that only one orientation of the lamellae is existing in the crystal; the white arrows highlight features from the UHMW-PE substrate. Higher resolution b) topography and c) phase images obtained from the same crystal. The periodicity of the lamellae is 5.4 ± 0.4 nm. The lamellae are better visualized in the phase images.

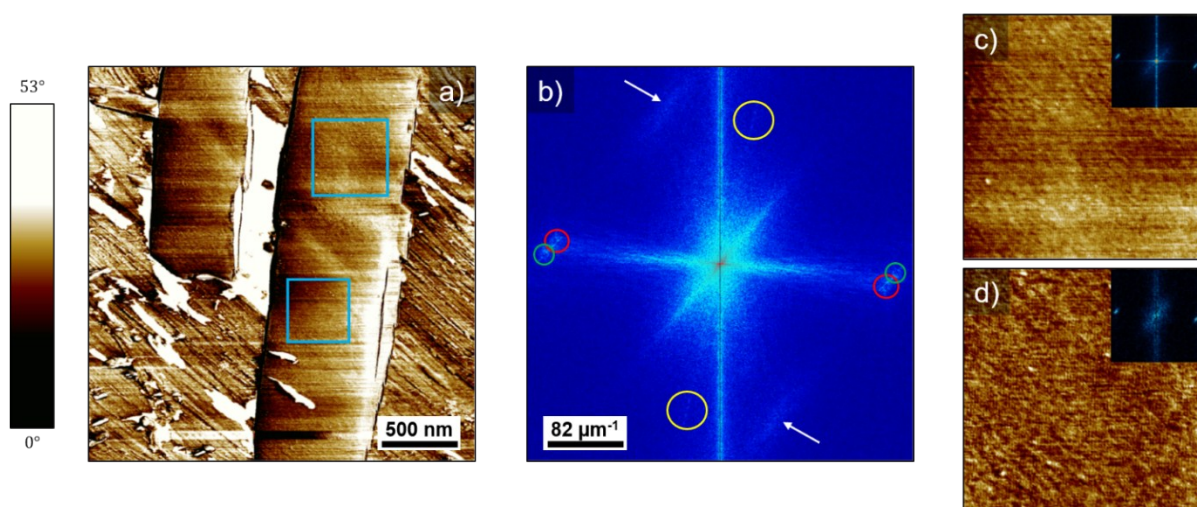


Figure S19: AFM images. a) Phase image of epitaxially grown crystals of **2** on UHMW-PE. No domain boundary is observed within the crystals, suggesting a single-crystalline nature. b) Fourier transform of the image in a). The bright dots highlighted by the red and green circles correspond to the lamellar periodicities of the big crystals on the right and left part of a), respectively. The tiny crystal on the top left part of the image also presents features in the Fourier transform, as highlighted by the yellow circles. The white arrows highlight features from the UHMW-PE substrate. c, d) High resolution phase images obtained from the regions highlighted by the blue squares on a) (c = top square, d = bottom one), with their Fourier transform in inset. They exhibit both the same orientation and a periodicity of 5.4 ± 0.4 nm, confirming the single-crystalline nature of the crystals.

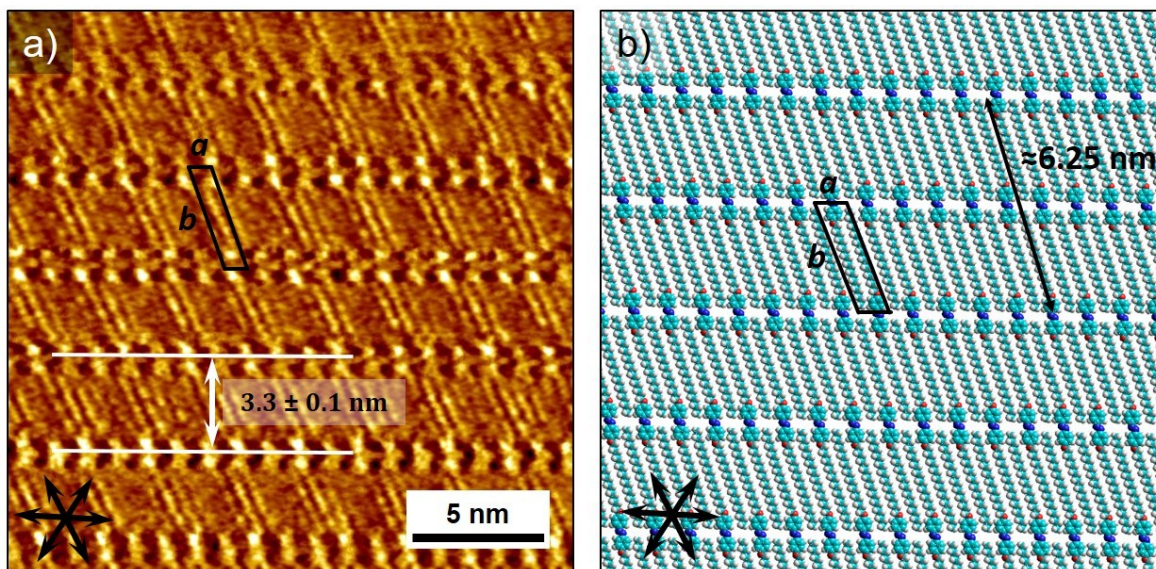


Figure S20: a) High-resolution STM image showing long-range ordered assembly of **1** (10^{-4} mol·L $^{-1}$) at the 1-PO/HOPG interface. The main symmetry axes of the HOPG lattice are shown in the lower left corner of the STM image. Imaging parameters: $I_{set} = 100$ pA, $V_{bias} = -1.2$ V. b) Proposed molecular model of the self-assembled monolayer of **1**. Unit cell parameters: $a = 1.0 \pm 0.1$ nm, $b = 3.5 \pm 0.1$ nm and $\gamma = 67 \pm 2^\circ$.

XRD data

To study the lattice orientation of the azobenzenes on drawn PE, wide angle X-ray scattering (WAXS) and grazing-incidence wide-angle X-ray scattering (GIWAXS) measurements were performed. WAXS patterns of the bilayer film with the incident X-ray perpendicular to the film are shown in Figure S17. The 110 and 200 reflections were used to calculate the lattice parameter of the orthorhombic unit cell of **1** and oriented PE (Figure S8). Figure 4b shows the middle angle X-ray scattering (MAXS) patterns of **1** crystallites on the UHMW-PE substrate. The 110 and the 200 spot are perpendicular to the **1** spot, corresponding to the epitaxies of **1**. In these figures, the PE c-axis is horizontal.³ The azobenzenes **1** and **2** form orthorhombic crystals with their chain axis parallel to the PE substrate with (001) azobenzene parallel (110) PE and (001) azobenzene parallel (001) PE. In general, the azobenzenes are oriented parallel to the PE and the b axis of the azobenzene unit cell is parallel to the c axis of PE. From the above results, we concluded that the epitaxial crystallisation of the azobenzenes on PE is based on the similar orthorhombic unit cell of the alkyl chains of **1** (a) 0.668, (b) 0.453 nm and drawn PE (a) 0.670, (b) 0.444 nm.

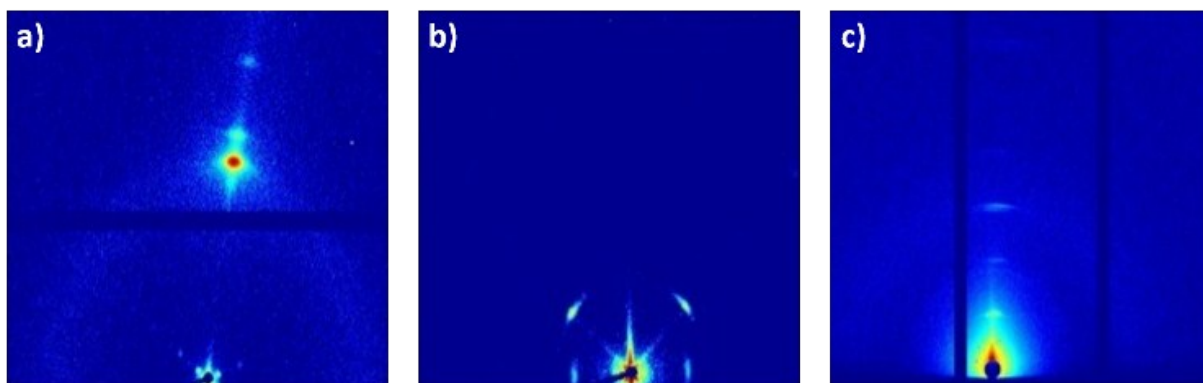


Figure S21: Crystallites of **1** on oriented UHMW-PE films a) 2D WAXS patterns, b) MAXS patterns, c) 2D GIWAXS patterns, the 2D map is recorded for the incident X-ray beam oriented perpendicularly to the drawing direction of UHMW-PE.

References

- 1 L. Shen, K. Nickmans, J. Severn and C. W. M. Bastiaansen, *ACS Appl. Mater. Interfaces*, 2016, **8**, 17549–17554.
- 2 B. Ilan, G. M. Florio, M. S. Hybertsen, B. J. Berne and G. W. Flynn, *Nano Lett.*, 2008, **8**, 3160–3165.
- 3 T. Okihara, A. Kawaguchi, M. Ohara and K. Katayama, *J. Cryst. Growth*, 1990, **106**, 318–332.